Investigation of Diesel Engine Distinctiveness Fuelled by Aegle Marmelos Pyrolysis Oil-CuO Nanoparticles-Diesel Modified Opus with the Aid of Infra-Red Thermal Images-A Novel Study

Baranitharan Paramasivam*[+]

Department of Automobile Engineering, SRM Easwari Engineering College, Ramapuram, Chennai.6000089. INDIA

Sakthivel R.

Department of Mechanical Engineering, Amrita school of engineering, Amrita Vishwa Vidyapeetham, Coimbatore.641112. INDIA

Anand Babu K.

Department of Production Engineering, National Institute of Technology, Tiruchirappalli.620 015. INDIA

Sasikumar R.

Department of Mechanical Engineering, Mahendra Engineering College, Mallasamudharam. Namakkal. 637503. INDIA

Bhuvanesh Kumar, M.[•]; Balaji, N.S.

Department of Production Engineering, National Institute of Technology, Tiruchirappalli.620 015. INDIA

ABSTRACT: *Nano particles-based catalysts are additives that can be used in green fuels to improve the characteristics of an engine. In the present study, non-edible Aegle Marmelos (AM) de-oiled seed cake biomass is used for the production of pyrolysis oil. The copper oxide (CuO) nanoparticles are prepared via the Sol-Gel process and categorized by Scanning Electron Microscopy (SEM), Energy-Dispersive X-Ray (EDAX) Spectroscopy, and Fourier Transform InfraRed (FT-IR) Spectroscopy. The CuO nanoparticles are mixed with pyrolysis oil-diesel opus at a fraction of 30 and 50 ppm. The Technique for Order Preference by Similarity to Ideal Solution (TOPSIS) tool is employed to attain the optimum engine process parameters. The correlation between cylinder head temperature and exhaust emission was concluded by using an innovative approach to thermography image processing. The outcomes of experimental, TOPSIS, and image processing revealed that modified fuel opus emitted a lesser amount of carbon monoxide, oxides of nitrogen, and unburned hydrocarbon compared with diesel but augmented CO_2 (Carbon dioxide) emission. It is found that higher CO_2 emission is apparent for the dynamic combustion process. This study confirms that AM bio-oil opus is an affordable alternate fuel for diesel engines for a clean and green environment.*

KEYWORDS: *Aegle marmelos bio-oil; Copper oxide nanoparticles; Engine performance; Engine emission; TOPSIS; Infrared Thermography.*

***** *To whom correspondence should be addressed.*
+ *E-mail: baraniparamasivam@gmail.com*
● *Other Address: Department of Mechanical Engineering, Kongu Engineering College, Erode.638060. INDIA*
1021-9986/2023/1/286-309 24/$/7.04

INTRODUCTION

The demand for energy sources has been an issue due to the exploitation of fossil fuels. Although fossil fuels are inevitable in the transportation sector, they emit harmful gases. The alternative to using fossil fuels involves using renewable sources of energy such as biofuels. [1]. Biofuels are the perfect solution to an environmentally friendly, long-lasting, and economical fuel to be used to overcome the energy crisis and in turn, develop the economy of the country [2]. Recently, the quest for biofuels has become very extensive due to the rising concern of exhaustion of natural resources. Bio-energy is now recognized as a potential alternative with the capability to contribute predominant non-conventional energy share shortly [3]. The production of biofuels involves the steps of processing biomass, which refers to solid agricultural wastes [4]. Considering the different energy conversion processes, pyrolysis is the most recognized owing to the superior bio-oil yield along with char and syngas [5]. The process of pyrolysis refers to the thermal disintegration of feed into its elementary components in the absence of oxygen [6]. Generally, biodiesel is oxygenated, hence engines can have more complete combustion than ordinary diesel and can lead to lower emissions [7]. Biofuel is considered a 'carbon neutral' fuel because the amount of CO_2 absorbed during growth is equal to the amount that is released during its combustion. Every biomass materials have individual fuel characteristics [8]. Since the properties depend on the plantation conditions and the richness of the soil, the quality and quantity of the biofuel produced from it primarily depend on feedstock characteristics and the efficiency of the processing steps [9]. Nanoparticles (particle size less than 100 nm) have a higher magnitude of upper heat transfer coefficient while transferring heat instantly to the surrounding fluid [10]. So, the addition of nanoparticles in diesel can increase conductivity [11]. Nanoparticles possess a large surface area-to-volume ratio, so they can react very quickly [12]. This makes them useful catalysts to speed up the reactions [13]. The nanoparticles have substantial benefits and create no blockage in the fuel filter and injector [14].

Fu et al. (2017) investigated the influence of adding 50 ppm of $Ce_{0.7}Zr_{0.3}O_2$ as a nanocatalyst in corn stalk pyrolysis oil/diesel blends. They have reported 8.4% fuel saving and 20% reduction in UHC, CO and NOx emissions [2]. Kumaravel al. (2019) tested the influence of CeO_2 as a nano additive for tyre oil-diesel blend. They concluded that the blend B5D85 +CeO_2 100 ppm has shown improvement of the BTE in the magnitude of 2.94% and reduction of harmful emissions by 7.46% compared with diesel at peak load [4]. Karthikeyan and Prathima (2016) examined the effect of CeO_2 nano additive in Prosopis juliflora biodiesel blends in the range of 50-100 ppm. The author revealed that the addition of CeO_2 diminished the CO, UHC, and NOx emissions compared to a plain B20 blend [14]. *Sharma et al*. (2016) investigated the effect of 100 ppm of carbon nanotubes (CNT) and CeO_2 in the tire pyrolysis oil (TPO) and Jatropha methyl ester (JME) opus-powered CI engine. At peak load condition, JME80TPO20, JME80TPO20$CeO_2$100, and JME80TPO20CNT100 blends depict that BTE of 24.25 to 25.64 % was augmented with CNT+ CeO_2 nano additives. Additionally, UHC, NOx , CO and smoke emissions were recorded lesser related with JMETPO [15].

Sachuthananthan et al. (2019) assessed the effect of MgO nanoparticles mixed with plastic oil (PPO) on the engine characteristics. They have observed that PPO mixed with 75ppm MgO nanocatalyst enhanced the BTE by 2.5 % and lower CO and UHC emissions reduced up to 5% [16]. *Gumus et al*. (2016) studied the effects of Al_2O_3 and CuO nano additive (range of 25 to 100 ppm) over neat diesel on the engine characteristics. The author concluded that the nano-diesel modified fuel blend improved the engine performance and decreased the CO, UHC, and NOx exhaust emission [17]. *Tamilvanan et.al* (2019) performed the engine investigation on a single-cylinder direct injection diesel engine, using modified biodiesel attained from Calophyllum inophyllum oil. The author found that the incorporation of copper nanocatalyst enhanced the BTE and decreased BSFC compared to other biodiesel blends but not better than diesel. The NOx, UHC, and CO emissions are reduced, whereas CO_2 emission is increased for copper nano-additive opus compared with diesel [18].

Optimization methods provided greater engine operating parameter combinations that were found to be efficient and effective by the researchers [19, 20]. The TOPSIS system was developed by *Hwang* and *Yoon* [21, 22]. It is an efficient, simple and effective multi-objective decision-making technique to obtain an optimum outcome among the alternatives [23]. Among the optimization techniques, TOPSIS received superior attention from researchers owing to their good computational techniques,

qualitative judgments, effective decision-making approach and simple mathematical formation [24, 25]. It can measure the relative performance for each alternative and can solve various real-time hitches [26, 27].

Anupam et al. (2014) optimized the selection of feedstock material for pulp and paper making processes via the TOPSIS tool. They have selected the different types of Eucalyptus species for this study through physicochemical characteristics, pulp characterization, cooking experiments and chemical morphological analysis assessment. It was concluded that E. citriodora was elected as the most suitable species for pulp and paper-making processes [28]. *Muniappan* and *Rajalingam* (2018) optimized the effect of intake charge temperature and EGR using TOPSIS in engine characteristics. They recorded that the CI (compression ignition) engine with 320 K charge inlet temperature delivered enhanced BTE of 28.6% whereas CO and UHC emissions were decreased up to 0.025% and 12.5 ppm respectively. The harmful NOx emission was diminished up to 240 ppm for 30% Exhaust Gas Recirculation (EGR) [29]. *Madhu et al.* 2018 investigated the best feedstock quality to obtain greater bio-oil yield during the pyrolysis process. They selected the five biomass materials such as sunflower shell, rice straw, hardwood, palm shell, wheat straw for which volatile matter, cellulose, hemicellulose, lignin, fixed carbon, ash, moisture were considered as control factors for this study by employing TOPSIS technique. The author concluded that a great volatile matter presence (79.2 wt%) of hardwood feedstock was nominated as the suitable feedstock material [30].

Among the measuring systems used Infrared Thermography (IRT) is one of the non-contact temperature measuring methods. IRT is a frequently used method as it can detect hidden surface heat and present accurate results of heat liberation data [31, 32]. The system works by releasing InfraRed (IR) radiation from a hot area at a temperature above absolute zero [33, 34]. Doing so helps in translating invisible heat which is captured in a visual thermal image where the amount of thermal energy released from an object can be detected, which makes it a useful method for real-time temperature monitoring [29]. The captured image can be transformed into analog signal and then to temperature values using special optical configurations in the lens of the IR camera which produces a 2D image. Its rapid capturing speeds make it a suitable measuring method for testing huge areas with complex geometries [35].

Ramesh et al. (2019) experimentally investigated the impact dampers attached to a boring tool. They assessed the tool temperature using IRT images. Using the thermal images results the optimal cutting conditions were evaluated in their research [33]. In the research conducted by *Shameer* and *Ramesh* (2017), they examined the CI engine characteristics fuelled with different biodiesel opuses. The association of the cylinder temperature and oxides of nitrogen magnitude was studied using IRT. They concluded that the combustion temperature is a important criterion for the amount of NOx produced during the combustion using their thermal image study data [35]. *Peer* and *Peer* (2019) studied the characteristics of the diesel engine when powered oil is obtained from pyrolysis of waste plastics. It was observed during their research that a lower BSFC and BTE along with higher CO assisted in augmenting the plastic oil blend ratio. The emission of NOx was observed at the exhaust port which was linked with a thermal image study of the cylinder of the engine. They confirmed the existing correlation between combustion temperature and NOx emission [36].

Kibar Murat Efgan and *Akin Ayse Nilgun* (2021) optimized the parameters (temperature during the reaction, concentration of sodium metaborate, flow rate of carbon dioxide, and the molar ratio of sodium metaborate/sodium hydroxide) which affect the carbonation reaction of CO_2 with sodium metaborate solutions. The authors concluded that the rate of consumption of CO_2 was 0.80 mol CO_2/min at optimum, which is coherent with the experimental mean value of 0.77 mol CO_2/min [37]. *Nwosu-Obieogu Kenechi et al.* (2021) optimized the rubber seed oil epoxidation process parameters using Response Surface Methodology (RSM). The authors found that the optimal condition for the predicted oxirane value, 1.5333%, was obtained at a reaction time of 6.49 hours, a stirring speed of 667.26, anda catalyst concentration of 1.82 mol [38].

From the literature review, it is evident that no investigation has been reported on the assessment of performance and emission behaviour of CI engine using AM bio-oil-diesel-CuO nanoparticles additive opus as of today. To the best of the authors' knowledge, only the TOPSIS technique has been involved to investigate the engine performance fuelled by pyrolysis oil with their blends. But the combination of both TOPSIS and

IR-thermography approaches for analysis of diesel engine characteristics were not yet carried out. To fill this research gap, the novel method of using a thermography imager for exploring the relationship between the cylinder head temperature and engine exhaust emission analysis has been evaluated with aid of TOPSIS in this study. Comparisons of the engine behaviour of the baseline diesel with and without the nano additive added fuel blend were also presented. In the present research era, it is unavoidable to resolve multi-criteria problems. In this view, TOPSIS and IR-image processing techniques were employed to optimize engine parameters and validate the exhaust port emissions respectively.

EXPERIMENTAL SECTION

Biomass

The AM tree is inborn of India which is abundant i n the sub-Himalayan forests and widely distributed throughout the world [39, 40]. The AM tree is a moderately growing, medium-sized tree, which has a place with the Rutaceae family [41, 42]. The AM fruit seeds contain almost 50% of oil content. It can survive in assorted soil conditions, is tolerant to waterlogging and has an unusually wide temperature resilience. De-oiled seed cake, a form of agricultural residue, could be a potential source for the biofuel production [43]. The AM feedstock materials are collected from the oil extracted waste.

The elemental analysis is used to evaluate the biomass eminence [44]. The higher value of volatile matter (VM=74.12%) describes that the feedstock material is appropriate for pyrolysis [6]. The VM of biomass is disintegrated into short-chain organic vapour during the pyrolysis [43]. The lower fixed carbon (FC=20.97%) depicts the potential of seed cake quality for the pyrolysis process. A lower amount of moisture (M=2.76%) showsthe suitability of AM biomass as solid fuel. T he lower amount of ash (A=2.15%) in seed cake material is essential according to the soil and plantation conditions.

The elemental analysis was conducted as per the (American society for testing and materials) ASTM D5291-96 standard. A Perkin Elmer 2400 Series II CHNSO elemental analyser was employed to perform the investigations to obtain the percentage of hydrogen (H), carbon (C), oxygen (O), nitrogen (N) and sulphur (S) content [5]. The ultimate analysis depicts that the AM biomass can be efficiently used as a feedstock in the thermochemical conversion method. The elemental composition of AM biomass is represented in Table 1.

Pyrolysis method

Fig. 1 portrayed the pyrolysis reactor. The experiment was conducted in a fixed bed reactor where the furnace temperature is maintained constant using a PID controller connected with thermocouple. The outlet of the reactor was coupled with a condenser to collect the vapour produced during the pyrolysis process.

Raw feed was filled in the reactor of 2 kg and was sealed to prevent environmental interactions. When the reaction starts, vapor comes out of the pyrolysis reactor through the outlet and is condensed. Water is used as a cooling medium for the condenser and circulated using a pump. The condensed vapor is collected in a suitable container as pyrolysis oil whereas the non-condensable gases were simply left out.

Copper nanoparticles synthesis

Fig. 2 exposes the synthesis of CuO nanoparticles. The CuO nanoparticles are given attention due to their unique properties as well as excellent optical and electrical performances [18]. The addition of CuO nano solid particles in diesel can enrich the conductivity and donate oxygen [17]. The CuO nanoparticles exhibit a narrow bandgap of about 1.2–1.9 eV. In this study, the synthesis of CuO is performed by the Sol-Gel approach because this process is economical and easy. The aqueous solution of $CuCl_2 \cdot 2H_2O$ (0.2 M) is prepared in a cleaned round bottom flask. The previous aqueous solution was added to 1 mL of glacial acetic acid and heated to 100 °C with constant stirring. Further, 8 M NaOH is added to the previously heated solution till pH reaches 7.

The green solution turns black instantly and black precipitate was seen. The obtained black precipitate was centrifuged and washed 3-4 times using de-ionized water. It was dried in an oven for 24 hours. The prepared powder is further used for characterization. The chemical reaction involved in the process is:

Figs. 3-5 portrayed the confirmation test of CuO nanoparticles. SEM is used for examining topographies of specimens at large size magnifications. The morphological studies of synthesized nanoparticles confirm the presence of copper nanoparticles with a size of around 15-30 nm. The FT-IR frequency absorption results reveal that the O-H

Table 1: Elemental analysis of AM de-oiled cake.

Proximate analysis* (wt%)				Ultimate analysis* (wt%)					
FC	VM	A	M	C	O	N	S	H	CV
20.97	74.12	2.15	2.76	47.87	43.69	2.85	0.01	5.58	20.21

**Dry basis*

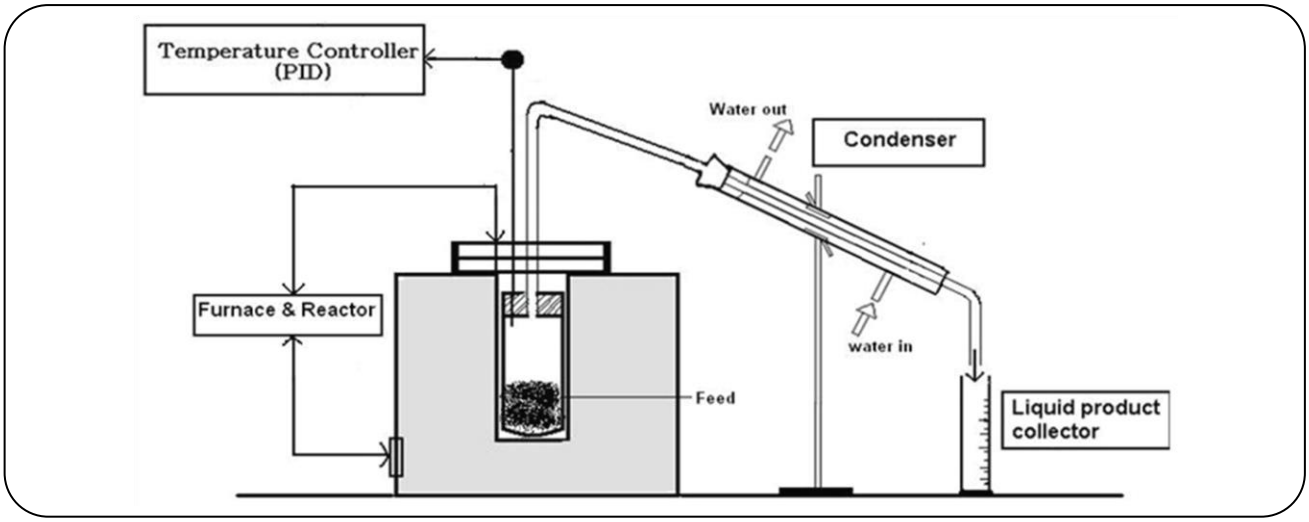

Fig.1: Thermochemical conversion reactor.

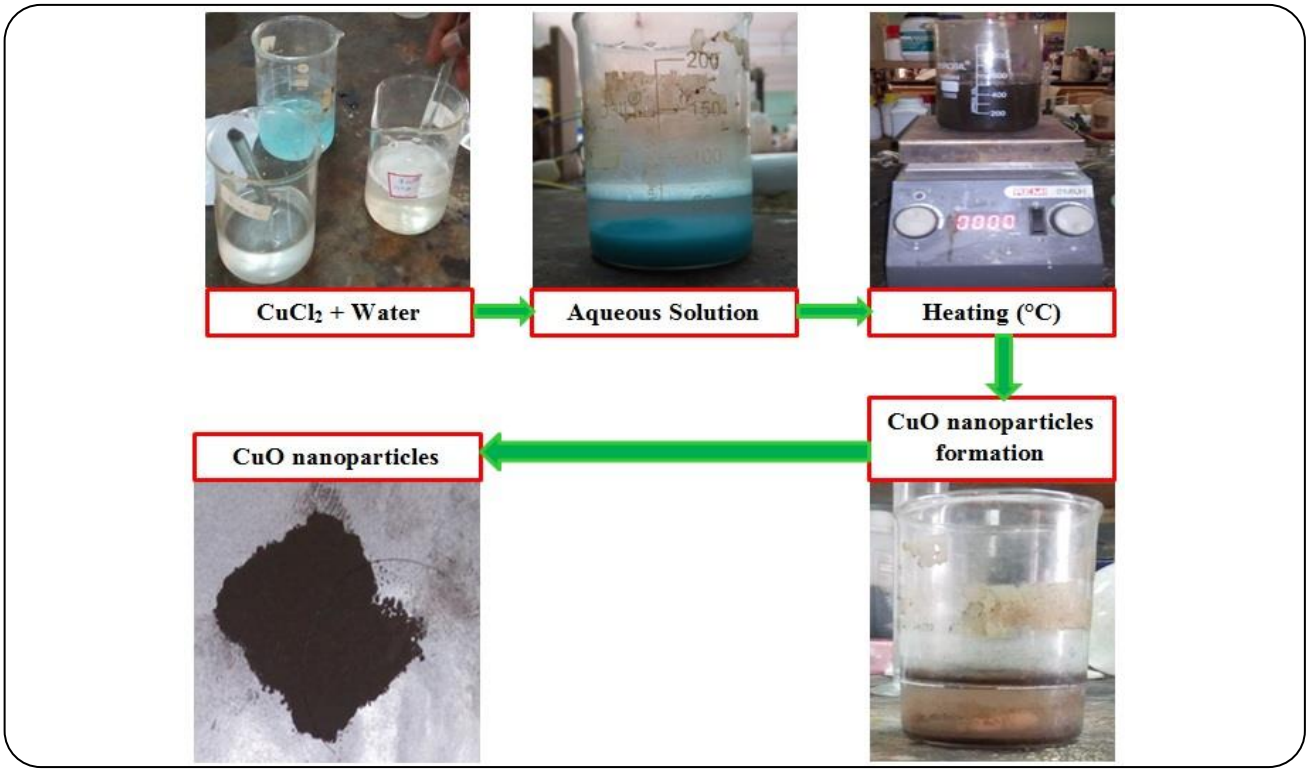

Fig.2: Copper nanoparticles synthesis process.

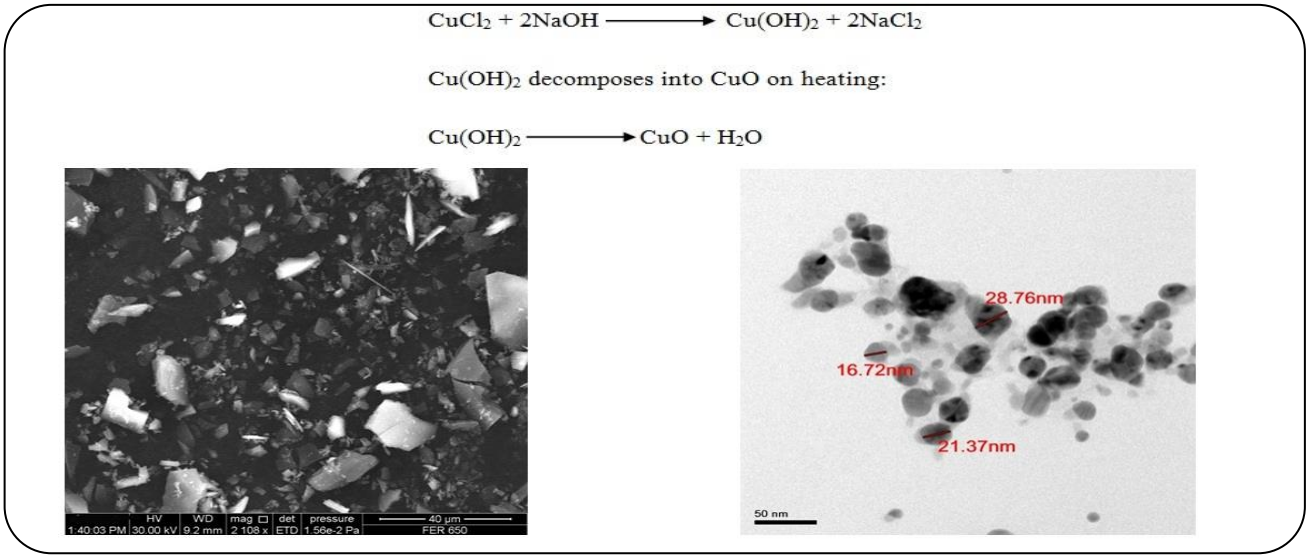

Fig. 3: SEM analysis of CuO nanoparticles.

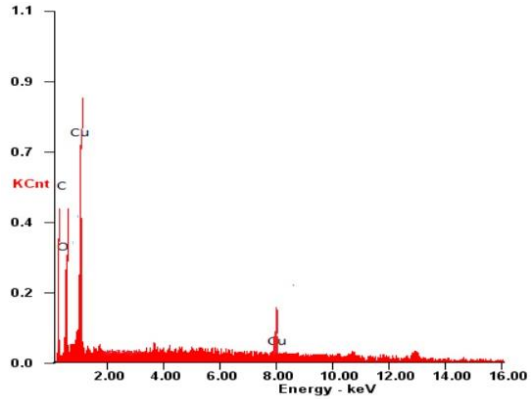

Fig. 4: EDAX analysis of CuO.

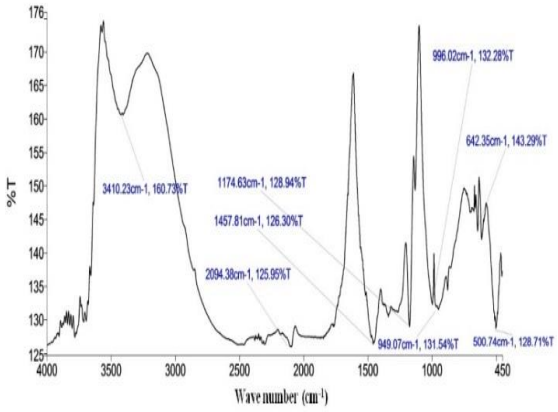

Fig. 5: FT-IR spectrum of CuO.

stretch at 3410.23 cm^{-1} shows the presence of an aliphatic primary amine. The methyl group compound C-H stretch frequency was detected at 1457.81 cm^{-1} band region. The spectrum region of 600-480 cm^{-1} illustrated the presence of Cu-O bond formation. The FT-IR spectroscopic frequency analysis endorses the formation of CuO nanoparticles. The SEM, EDAX, and FT-IR analysis ensured that the resultant particles were formed from the Sol-Gel process.

Test engine setup

Fig. 6 shows the engine test rig line-up used in present research. A single-cylinder direct-injection multi-fuel test engine combined with an Eddy Current DynamoMeter (ECDM) was used in this investigation. An ECDM was employed to apply the prerequisite engine load (W) with a digital DAQ system.

The DAQ is prompt for the test, which controls the process by including data logging, and in-vehicle monitoring. Primarily, the engine was started with baseline fuel (F0), and warmed up at no load. Subsequently, the engine analysis was conducted at standard operating conditions with different test fuel opus (F1, F2, and F3). Consequently, the mandatory data was collected. Each engine data reading was repeated thrice to attain a mean average value. The CI engine connected with AVL 250 modular diagnostic system was used to observe the engine's emissions during the operation. The specification test engine and emission AVL analyser is same as that of our previous research work [24].

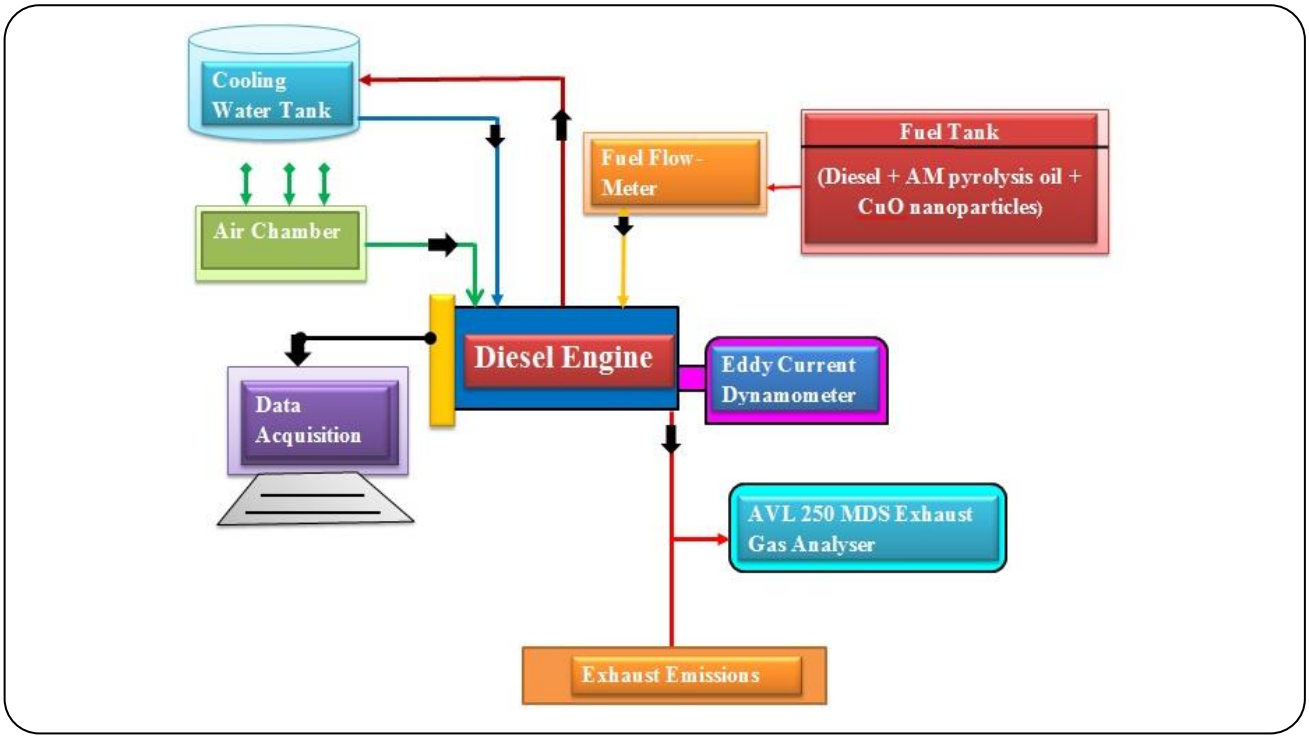

Fig. 6: Test engine setup.

Thermal imager

In this study, a FLUKE Infrared-Thermal imager was employed to analyze the in-cylinder temperature during engine operation. The basic principle of an IR-thermal imager is transferring the IR energy released by the hot surface into thermography with numerical data of the required object [45]. A thermal imager (TIM) was focused on the engine cylinder with the help of a spotlight at the preferred spot. The TIM sense the IR energy during engine operation and offers the heat delivery of the cylinder head [35]. Thermal images are taken manually at the necessary engine load (W) with various modified fuel blends and stored in external memory for further investigation.

Technique for order preference by similarity to ideal solution

TOPSIS technique is a Multi-Criteria Decision Making (MCDM) technique to find an enhanced optimum solution among a large number of alternatives [30]. It was developed based on the idea that the chosen alternatives have the least distance from Positive Ideal Solutions (PIS) and higher distance from Negative Ideal Solutions (NIS) for resolving the MCDM problem [22]. In TOPSIS, the PIS is a gathering of the highest values, whereas the furthest ideal outcomes are attained by the lowest values attainable for the criteria [21]. It is an efficient and simple MCDM technique used in several real-time applications. In this method, all the outcomes are separated into favourable or non-favourable characters [28]. The greater attributes are referred to be favourable characters and the poorer attributes are referred to be non-favourable characters [29]. The process to select the greatest alternative by using TOPSIS techniques includes the following step by step procedure:

Step 1: Primarily, the decision matrix (Da) should be developed using all the obtained experimental outputs. The decision matrix consists of 'b' attributes and 'a' alternatives. In the present study, experimental trials are the alternative solutions (a) and the outcomes are the attributes (b) [21]

$$Da = \begin{bmatrix} x_{11} & x_{12} & x_{13} & \cdots & \cdots & x_{1j} \\ x_{21} & x_{22} & x_{23} & \cdots & \cdots & x_{2j} \\ \vdots & \vdots & \vdots & \vdots & \vdots & \vdots \\ x_{i1} & x_{i2} & x_{i3} & \cdots & \cdots & x_{ij} \end{bmatrix} \quad (1)$$

Where X_{ij} is the measure of the j^{th} attribute to the i^{th} alternative. i=1,2,3,…….,a and j=1,2,3,……,b.

Step 2: The normalization of the TOSIS design matrix was computed by the following Equation (2) [29]

$$\delta_{ij} = \frac{X_{ij}}{\sqrt{\sum_{i=1}^{a} X_{ij}^{\,2}}} \quad (2)$$

Where, δ_{ij} is normalized value for i=1,2,3,……..,a; j=1,2,3,……b.

Step 3: The weights of every attribute are allotted and the sum of the weights of all attributes should be equal to one. The weighted normalized matrix (ϕ_{ij}) is computed as follows [28]

$$\phi_{ij} = W_j \delta_{ij} \quad (3)$$

Where, $\sum_{j=1}^{b} W_j = 1$

Step 4: Identification of positive ideal solution (PIS=ϕ^+) and negative ideal solution (NIS=ϕ^-) are computed by following equations (4) and (5) [21]

$$\phi^+ = (\phi_1^+, \phi_2^+, \ldots\ldots\ldots, \phi_b^+) = \{(\max \phi_{ij} / j \epsilon J_1), \quad (4)$$
$$(\min \phi_{ij} / j \epsilon J_2, i=1,2,3,\ldots\ldots\ldots,b)$$

$$\phi - = (\phi_1^-, \phi_2^-, \ldots\ldots\ldots, \phi_b^-) = \{(min\ \phi_{ij} / j \epsilon J_1), \quad (5)$$
$$(\min \phi_{ij} / j \epsilon J_2, i=1,2,3,\ldots\ldots\ldots,b)$$

Where, J_1=set of favourable attribute and J_2=set of non-favourable attribute

Step 5: The positive separation measures (S_i^+) and negative separation measures (S_i^-) of every alternative are calculated by following Equations (6) and (7) [30]

$$S_i^+ = \sqrt{\sum_{j=1}^{b} (\phi_{ij} - \phi^+)^2} \quad (6)$$

$$S_i^- = \sqrt{\sum_{j=1}^{b} (\phi_{ij} - \phi^-)^2} \quad (7)$$

Where, i=1, 2, 3…… a.

Step 6: The assessment of the Relative Closeness Coefficient (RCC) of every alternative is computed as follows [21]

$$RCC = \frac{S_i^-}{S_i^+ + S_i^-} \quad (8)$$

Where, i=1,2,3,……x.

Step 7: Based on the performance value of RCC, every alternative is ranked in the descending order manner. The main value is ranked in the first position and the smallest value is ranked in the last rank.

Instruments uncertainty analysis

The instrument accuracy is exposed by conducting an uncertainty analysis. Errors and uncertainties arise during experiments depending on the instrument's periodic calibration, instrument selection, method of data observation, working condition, and environment [6]. Accuracy and perfection determine the consistency of experimental precision of the instruments [7]. Table 2 represents the accuracy and uncertainty of the measuring instrument used in this research. The uncertainty of the instrument used during the investigation was computed by the following equation.

$$\text{Overall uncertainty} = \sqrt{\left(\frac{\Delta X1}{X1}\right)^2 + \left(\frac{\Delta X2}{X2}\right)^2 + \left(\frac{\Delta X3}{X3}\right)^2 + \cdots + \left(\frac{\Delta Xn}{Xn}\right)^2}$$

Where ΔX→ accuracy of the measuring instruments; X1→ experiments output response; $\left(\frac{\Delta X1}{X1}\right), \left(\frac{\Delta X2}{X2}\right)$ → independent variable errors; S→ estimated quantity; X1, X2, X3……Xn→ value of estimate quantity error.

$$\text{Overall certainty} = \sqrt{\begin{matrix}(0.4)^2 + (0.006)^2 + (1.2)^2 + (0.1)^2 + (0.25)^2 + (0.15)^2 + (0.65)^2 + (0.2)^2 + (0.05)^2 \\ +(0.32)^2 + (0.2)^2 + (1)^2 + (0.2)^2 + (1)^2 + (1.12)^2\end{matrix}}$$
$$= 2.3\%$$

RESULTS AND DISCUSSION

Test fuels preparation and properties

Conferring to the Indian biofuel policy (2017), the estimated amalgamation of biofuel can go up to 20% [6]. For test fuel preparation, initially, 20% of AM bio-oil, 80% diesel, and less than 1% of surfactants by volume basis were mixed using stirrer at ambient temperature [2]. Subsequently, AM pyrolysis oil+diesel altered fuel blends were dosed with CuO nanoparticles in the range of 30 ppm and 50 ppm. Nano-bio-oil blends were prepared by using an ultrasonicator. It is a novel fuel which is consists of CuO nanoparticles, AM pyrolysis oil and diesel. The following modified fuel opus was prepared for physicochemical property studies and engine tests as follows: F0=Diesel; F1=20% of AM bio-oil oil+80% of diesel; F2=20% of AM pyrolysis oil+80% of diesel+30 ppm CuO nanoparticles; F3= 20% of AM bio-oil+80% of diesel+ 50 ppm CuO nano particles.

The physicochemical characteristics of fuel mixtures were obtained as per ASTM standards. The CV values of all modified blends (F1, F2, and F3) were less compared

Table 2: Measuring instruments and Uncertainty.

Instruments	Parameters measured	Accuracy	Uncertainty (%)
PerkinElmer 2400 series II CHNSO elemental analyzer	Analyse the percentage of C, H, S, N and O in sample (weight %)	±0.3%	±0.40
PerkinElmer Spectrum FT-IR SP 10S/W spectrophotometer	Analyse the functional group of compounds present in sample (wavelength in cm^{-1})	±0.1 cm^{-1}	±0.006
EDX scanning spectrometry detector	Analyse the elemental composition of the sample (weight %)	±5%	±1.2
Thermocouple	Determine the reactor temperature (°C)	±1 °C	± 0.1
Density meter	Determine the density of the sample (g/cc)	±0.01 g/cc	± 0.25
Kinematic viscometer	Determine the kinematic viscosity of the sample (cSt)	<3% cSt	± 0.15
Ignition quality tester	Determine the cetane number of the sample	±1	± 0.65
Bomb calorimeter	Determine the calorific value of the sample (kJ/kg)	±0.05 kJ/kg	± 0.20
Test engine	BTE	±0.5%	± 0.05
	BSFC	±0.05 kg/kW hr	± 0.32
AVL 250 MDS	CO	±0.02 % vol.	±0.2
	UHC	± 1.25 ppm	±1
	CO_2	± 0.5 % vol.	±0.2
	NOx	±5 ppm	±1
IR-Thermal imager	Temperature	±2 °C	±1.12

Table 3: Physicochemical properties of innovated fuel opus.

Properties	Unit	ASTM	F0	F1	F2	F3
Calorific value	MJ/kg	D240	45	43.53	44.12	44.85
Viscosity	cSt@40ºC	D445	3.9	4.8	4.8	4.8
Density	g/cc @30ºC	D4052	0.845	0.89	0.89	0.89
Water content	wt%	D1744	-	16.2	16.4	16.7
Cetane number	-	D976	50	50.3	51.2	51.2
Appearance	-	-	Yellow	Dark brown	Dark brown	Dark brown

to F0. The lower CV turns to increase the BSFC [8]. The viscosity and density properties greatly influence fuel spray characteristics [3]. The CuO nanoparticles addition increases the Cetane Number (CN) [14]. Augmenting CN of the nano-bio-oil blends (F1 and F2) leads to shortened ignition delay and thereby increases the heat-transfer rate of a modified blend than diesel [16]. The presence of water existance in the pyrolysis oil blends may reduce the combustion temperature, which reduces the NOx emission at the exhaust port [6]. A metal oxide nano additive in the bio-oil and diesel mixtures results in an up-gradation of the fuel properties [46]. The upgraded fuel opus exposes the opportunity of using it as an alternative fuel source. The properties of prepared test fuels are shown in Table 3.

Design of experiments

The present study adopted a Taguchi quality loss function for the experimental design. Taguchi offered the design of the experimental approach which is a systematic technique for optimizing the constraints with a lesser test [21]. It is a time-saving and cost-effective approach for optimizing

Table 4: Engine process parameters and their levels.

Factors		Levels			
		I	II	III	IV
Engine load (%)	W	25	50	75	100
Fuel blend	F	0	1	2	3

Table 5: Engine output response.

Test No.	W	F	BSFC	BTE	CO	UHC	CO2	NOx
	%		kg/kW hr	%	%	ppm	%	ppm
1	25	F0	0.58	10.99	0.81	315	3.73	812
2	25	F1	0.63	11.13	0.71	281	3.76	738
3	25	F2	0.61	11.24	0.65	252	3.98	686
4	25	F3	0.59	11.31	0.52	239	4.11	564
5	50	F0	0.46	16.15	0.52	280	5.01	782
6	50	F1	0.51	16.87	0.48	258	6.1	692
7	50	F2	0.48	17.89	0.46	242	6.45	647
8	50	F3	0.47	18.01	0.36	221	6.93	537
9	75	F0	0.35	20.43	0.37	257	7.25	778
10	75	F1	0.42	21.94	0.34	246	8.42	676
11	75	F2	0.39	22.65	0.29	231	8.98	604
12	75	F3	0.37	23.76	0.27	201	9.12	528
13	100	F0	0.31	21.35	0.34	184	8.34	647
14	100	F1	0.36	22.32	0.3	167	9.36	558
15	100	F2	0.34	22.84	0.26	156	9.51	511
16	100	F3	0.32	23.97	0.24	143	9.78	487

the engine parameters. In this study, two process control factors with four levels of full factorial design have been adopted (2^4=2*2*2*2=16 test). The L_{16} orthogonal array is employed for this study with a minimum experimental test using Minitab 17 statistical tool. The current study focuses on two engine process control factors such as W (%) and innovated fuel blends according to the expert's advice and previous studies. The engine input factors and their levels are given in Table 4. The CI engine's emission and performance behaviour are measured under different W and modified fuel blends and the attained outcomes are represented in Table 5.

Engine performance analysis

Test engine performance behaviour such as BSFC and BTE was computed by following equations [3, 12]

$$\text{BSFC} = \frac{\text{TFC}}{\text{BP}} (\text{kg/kW h})$$

$$\text{Total fuel consumption, TFC} = \frac{\text{fv} \times 3600 \times \text{f}\rho}{\text{Time} \times 1000} \text{kg/h}$$

$$\text{Brake power, BP} = \frac{2\pi \text{NT}}{60 * 1000}$$

$$\text{BTE} = \frac{\text{BP} \times 3600}{\text{TFC} \times \text{CV}} \times 100\ (\%)$$

The BSFC for bio-oil blend, nano-bio-oil opus at various W conditions is illustrated in Fig. 7. Heat engine converts fuel chemical energy into mechanical energy [43]. The BSFC values for all fuel mixtures are high compared with neat diesel owing to the lower CV value of biofuel blends [7]. The lesser CV causes ineffective fuel burning. Generally, bio-fuel has a higher BSFC than diesel (F0) [37].

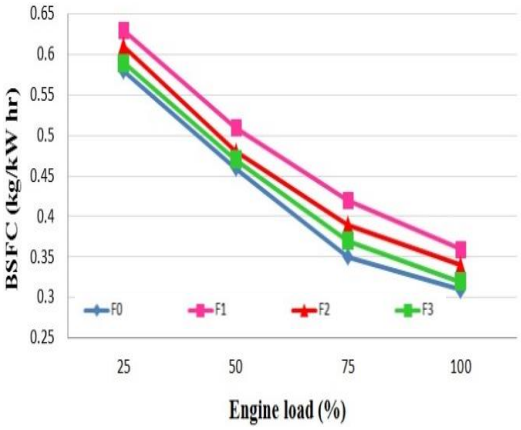

Fig. 7: BSFC.

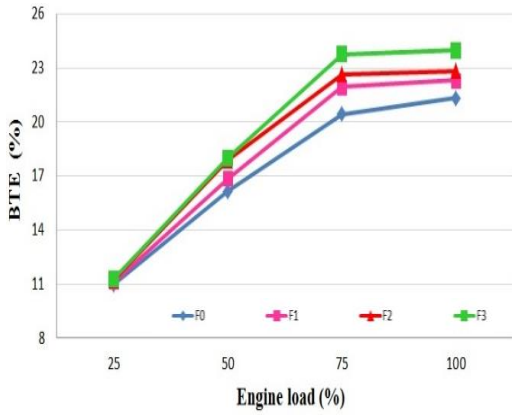

Fig. 8: BTE.

The bio-oil opus and nano-bio-oil opus have a lesser CV value, lesser heating value, higher density, and higher viscosity compared to F0. It results in longer ignition delay and inferior burning which leads to augmented BSFC value than F0 [13]. Henceforth, F1, F2 and F3 test fuels blends were recorded with augmented BSFC value than that of diesel. It is noticed that BSFC value had reduced significantly as the CuO nano additive concentration is raised in the fuel blends. The lower BSFC of 0.32 kg/kW-h has been obtained with F3 at 100% W, which is 0.31 kg/kW-hr for F0. It reveals that there is a marginal value of fuel consumption as compared with diesel. F3 has 2.94% higher BSFC than neat diesel but 13.71% lower BSFC than F1 and F2. The existence of higher oxygen in the nano additive fuel blend provided the enhanced fuel property which leads to a lower BSFC value [34]. From the BSFC graph, the non-additive F1 fuel opus has a more BSFC value of 0.36 kg/kW-hr at full load conditions. This is owed to the lesser energy content and slow-burning of F1 fuel.

Fig. 8 depicts the BTE significances of diesel, bio-oil blend and nano-bio-oil opus. BTE indicates how efficiently the engine can convert fuel chemical energy into mechanical energy [47]. At peak load conditions the more amount of fuel is sprayed at higher injection pressure [10]. The finest fuel atomization particles shorten the ignition delay and fuel velocity thereby improving the BTE [4]. The engine BTE value was increased with increasing CuO nano additive and augmenting W condition. This is due to the increasing in-cylinder pressure and temperature that lead to enriched combustion and result in a higher BTE value [15]. The surfactants emulsified with AM pyrolysis oil, diesel and CuO nanoparticles, cause the decreased value of viscosity and density of modified fuel blends, which tends to enhance the fuel atomization and spray properties [2]. Compared to F0 and other fuel blends, F3 shows the higher BTE at all engine loads. The maximum BTE of 23.97% is obtained for F3 fuel at 100% W, which is 21.35% for F0. This may be due to the amalgamation of oxygenated biofuel with metal oxide enhancing the fuel spray and atomization characteristics, which in turn increased in BTE value [16]. The lesser BTE of 11.13% has been observed for F1 at 25% of W. This is owed to insufficient fuel spray and oxygen deficiency of the F1 fuel.

Engine emission analysis

Fig. 9 showed the CO level for various fuels at different W. The CO emission is an intermediary product of the combustion process [35]. The CO emission is the former stage of the oxidation process later changes into CO_2 emission [7]. The deficiency of oxygen during the fuel burring causes CO emission [14, 48].

The rich air-fuel mixer delivers lesser CO emission at exhaust [17]. The deficient combustion, inadequate air/fuel mixer and insufficient oxygen supply of F1 fuel emit higher CO of 0.74% at 25% of load as compared to F0, F2 and F3. The CuO nanoparticles addition to bio-oil blends enriched the oxygen level which diminishes the CO emission [18]. A declining tendency was observed for CuO nano addition with AM pyrolysis-diesel opus. The minimum CO level was attained for F1 fuel of 0.24%, at full load, which is 0.34% for F0 fuel. This is due to the CuO nanocatalyst supplying sufficient oxygen

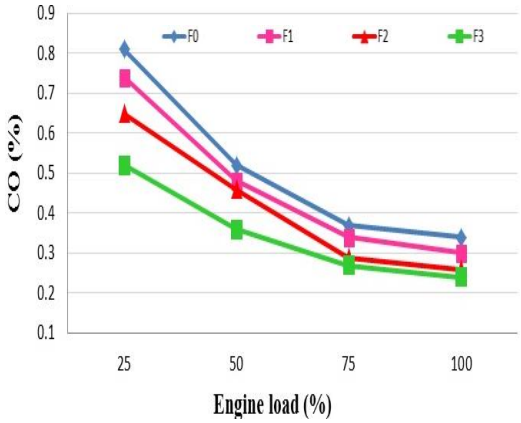

Fig.9: CO emission.

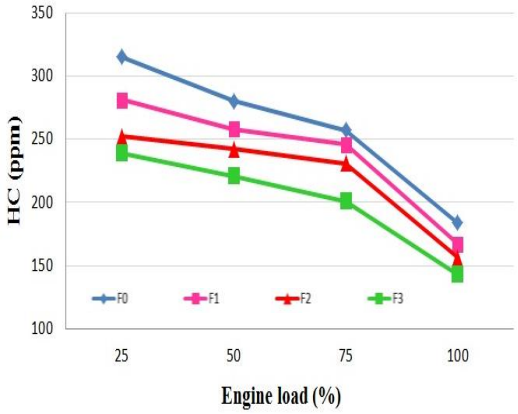

Fig.10: UHC emission.

to the nano-bio-oil blend, which lead to complete combustion, which in turn lowered the CO level.

Fig. 10 illustrates the emission of UHC for modified fuel opus. The increasing trend in CuO nanoparticles addition shows the decreasing tendency in the UHC level. The inadequate combustion of fuel packets in engine operation releases the UHC [6, 49]. The UHC emission is caused by unburnt fuel molecules present in the inside cylinder wall. At low loads, cylinder wall temperature and in-cylinder pressure were low [2]. Subsequently, sprayed fuel particles reaching the cool cylinder walls are dropped as unburnt fuel molecules. This leads to an augmenting UHC emission [7]. In the case of higher load, cylinder wall temperature and inside pressure was increased, which leads to complete combustion and reduces the UHC emission [17]. It should be noted that nanocatalyst enriched the combustion process thereby leading to complete fuel burning. F3 fuel emits a lesser UHC level than F0 and other modified blends. The lesser UHC emission is attained in F3 of 143 ppm at full load, which is 184 ppm for F0. The higher level of UHC emission was detected in F1 (281 ppm) at 25% of W, which is attributed to incomplete combustion, poorer fuel spray and distinctive fuel droplets.

Fig. 11 represents the CO_2 emissions of F0, F1 and nano-bio-oil blends. The higher amounts of CO_2 level at exhaust depict the complete combustion process [18]. The decrease in CO level may cause amplification of CO_2 emission at the exhaust. This is because of the sufficient amount of oxygen available in fuels resulting in the oxidation of CO into CO_2 [4, 50]. Compare to baseline fuel, all the modified fuel blends emit higher CO_2 at all loading conditions. This is caused by the complete combustion of oxygenated biofuels.

The non-nano additive blend F1 emits a lower CO_2 level compared to the nano-bio-oil opus. This is the fact that metal oxide CuO nanoparticles supplied an adequate amount of oxygen to fuel blends, which causes complete fuel combustion [2]. An F2 and F3 fuel emit the CO_2 level of 9.51% and 9.87% at 100%W, which is 8.34% for diesel fuel. The increased CO_2 level is observed for F3 compared to all test fuels. The lesser CO_2 value is detected for F1 test fuel, owing to insufficient oxygen supply and inadequate burning of fuel compared to nano-bio-oil blends.

Fig. 12 shows the tendency of NOx with respect to load for all test fuels. In general, higher load elevates the combustion temperature thereby shooting the NOx level high (Zeldovich mechanism) [8]. But the NOx is reduced by adding pyrolysis oil to test fuel blend. This can be because the water that exists in the pyrolysis oil reduces the flame temperature and causes a quenching effect [6, 51]. However, CuO oxygenated metallic nanocatalyst enhanced the flame velocity and fuel burning, which shortened the ignition delay with a high fuel burning rate. This causes complete combustion at lesser combustion temperature thereby minimizing the NOx emission level [14]. The lower NOx of 487 ppm was noted for F3 nano-bio-oil blend at full load which is 647 ppm for F0 blend. A similar decline NOx trend was recorded in literature studies [17, 18].

In the TOPSIS approach, initially, the entire experimental data are formed into a decision matrix form (Da) [19]. It consists of alternatives in rows (experimental test) and attributes in columns (experimental output response).

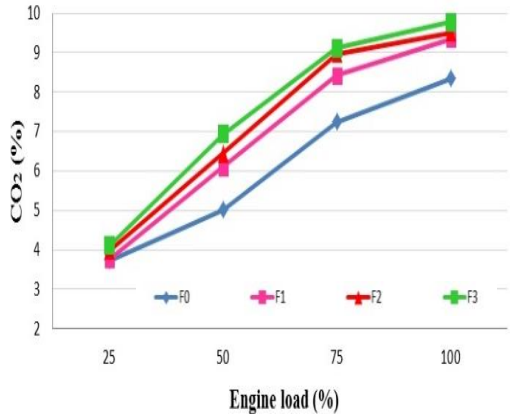

Fig.11: CO_2 emission.

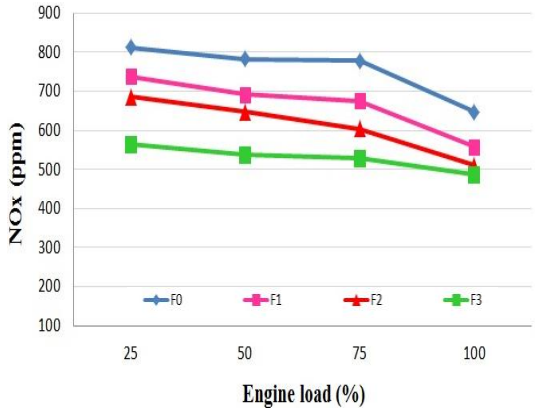

Fig.12: NOx emission.

TOPSIS outcomes evaluation

The 'Da' is normalized by using Eq.(2). Afterwards, relative weights are allocated to every attribute. Each outcome such as BSFC, BTE, CO, UHC, CO_2, and NOx was given equal importance [29]. Relative weight of 1/5 is allocated to every output response by using Eq.(3). The PIS and NIS are computed by Eqs. (4) and (5) correspondingly. Considering the output responses, PIS has higher values, which are ϕ^{+}_{BSFC} =0.03358, ϕ^{+}_{BTE} =0.06343, ϕ^{+}_{CO} =0.02608, ϕ^{+}_{HC} =0.03061, ϕ^{+}_{CO2} =0.06738, and ϕ^{+}_{NOx} =0.03240, whereas NIS has lesser of weighted normalized values are ϕ^{-}_{BSFC}=0.06825, ϕ^{-}_{BTE} =0.02908, ϕ^{-}_{CO} =0.08802, ϕ^{-}_{HC} =0.06742, ϕ^{-}_{CO2} =0.02570, and ϕ^{-}_{NOx} =0.05402. The separation measures of PIS (S_i^{+}) and NIS (S_i^{-}) are calculated by Eqs. (6) and (7). The final step of RCC was calculated by Eq.(8), and all alternative is ranked in descending order. Tables 6 and 7 illustrates the TOPSIS results. The lists of favourable and non-favourable attributes are presented in Table 8.

In TOPSIS analysis, the highest RCC value is nominated as an optimal result [21]. Test trial 16 has a higher RCC value of 0.988822 among all test trials. From this study, optimal engine parameters for nano-bio-oil powered engines are 100% W, and F3 fuel blend (20% of AM bio-oil+80% of diesel+50 ppm CuO nanoparticles).

Thermal image validation

The heat inside the combustion chamber flows through the exhaust and cylinder head. Once the engine is started, combustion temperature increases with augmenting engine load (W), consequently, the temperature of engine components is also elevated [36]. Compared to contact measurements, a non-contact measuring method delivers precise values [45]. The in-cylinder temperature was confirmed by an IR-thermal imager by assessing the temperature of the cylinder head temperature. The thermography images expose the heat distribution around the cylinder head [35]. Figure 13 elucidated the location of the thermal image capture for cylinder head temperature. Fig. 14 interpreted the cylinder head temperature of F0, F1, F2 and F3 fuel blends at different engine load conditions. Figs. 14.1, 14.5, 14.9, and 14.13 shows the same results for diesel fuel. Additionally, Figs. 14.2, 14.6, 14.10, and 14.4, shows the respective temperature for non-CuO nano additive pyrolysis oil. Figs. 14.3, 14.7, 14.11, and 14.15 portrayed the cylinder head heat distribution of the F2 blend, whereas Figs. 14.4, 14.8, 14.12, and 14.16 are inferred the same for F3 fuel. The temperature is captured from the cylinder head of the test engine. In thermography images, the head temperatures are labelled, conferring to the representations as "MAX", "AVG", and "MIN". The "MAX" and "MIN" denotes the higher and lower head temperature, whereas "AVG" indicated the average value of cylinder head temperature. The oxides of nitrogen emission depend on the combustion temperature.

The water existing in the pyrolysis oil blends (Water content of F1=16.2%, F2=16.4%, and F3=16.7%), decreases the combustion temperature, thereby reducing NOx level as compared with diesel. The same tendency was detected in previous studies [6, 12]. According to the thermography images analysis, the lesser cylinder head temperature was captured for the F3 (39° C) fuel blend at full load condition, which is 39.5° C for diesel. However,

Table 6: TOPSIS normalized and weighted average values.

Test No.	Normalized value						Weighted average value					
	BSFC	BTE	CO	UHC	CO_2	NOx	BSFC	BTE	CO	UHC	CO_2	NOx
1	0.3142	0.1454	0.4401	0.3371	0.1285	0.2701	0.0628	0.0291	0.0880	0.0674	0.0257	0.0540
2	0.3413	0.1473	0.3857	0.3007	0.1295	0.2455	0.0683	0.0295	0.0771	0.0601	0.0259	0.0491
3	0.3304	0.1487	0.3532	0.2697	0.1371	0.2282	0.0661	0.0297	0.0706	0.0539	0.0274	0.0456
4	0.3196	0.1496	0.2825	0.2558	0.1416	0.1876	0.0639	0.0299	0.0565	0.0512	0.0283	0.0375
5	0.2492	0.2137	0.2825	0.2997	0.1726	0.2601	0.0498	0.0427	0.0565	0.0599	0.0345	0.0520
6	0.2763	0.2232	0.2608	0.2761	0.2101	0.2302	0.0553	0.0446	0.0522	0.0552	0.0420	0.0460
7	0.2600	0.2367	0.2499	0.2590	0.2222	0.2152	0.0520	0.0473	0.0500	0.0518	0.0444	0.0430
8	0.2546	0.2383	0.1956	0.2365	0.2387	0.1786	0.0509	0.0477	0.0391	0.0473	0.0477	0.0357
9	0.1896	0.2703	0.2010	0.2750	0.2498	0.2588	0.0379	0.0541	0.0402	0.0550	0.0500	0.0518
10	0.2275	0.2903	0.1847	0.2633	0.2901	0.2249	0.0455	0.0581	0.0369	0.0527	0.0580	0.0450
11	0.2113	0.2997	0.1576	0.2472	0.3094	0.2009	0.0423	0.0599	0.0315	0.0494	0.0619	0.0402
12	0.2004	0.3144	0.1467	0.2151	0.3142	0.1756	0.0401	0.0629	0.0293	0.0430	0.0628	0.0351
13	0.1679	0.2825	0.1847	0.1969	0.2873	0.2152	0.0336	0.0565	0.0369	0.0394	0.0575	0.0430
14	0.1950	0.2953	0.1630	0.1787	0.3224	0.1856	0.0390	0.0591	0.0326	0.0357	0.0645	0.0371
15	0.1842	0.3022	0.1413	0.1670	0.3276	0.1700	0.0368	0.0604	0.0283	0.0334	0.0655	0.0340
16	0.1733	0.3171	0.1304	0.1530	0.3369	0.1620	0.0347	0.0634	0.0261	0.0306	0.0674	0.0324
						PIS	0.0336	0.0634	0.0261	0.0306	0.0674	0.0324
						NIS	0.0683	0.0291	0.0880	0.0674	0.0257	0.0540

Table 7: TOPSIS positive and negative separation measures with RCC.

Test No.	S_i^+	S_i^-	RCC
1	0.097118	0.006578	0.063434
2	0.088523	0.010684	0.107694
3	0.080576	0.020476	0.20263
4	0.070305	0.03623	0.340073
5	0.062794	0.038183	0.378133
6	0.054198	0.044075	0.448497
7	0.047521	0.050046	0.512939
8	0.037345	0.062648	0.626523
9	0.039751	0.065422	0.622044
10	0.031952	0.07067	0.688643
11	0.023719	0.079294	0.769745
12	0.015344	0.085559	0.847935
13	0.021327	0.078197	0.785707
14	0.012166	0.085003	0.874793
15	0.006165	0.090879	0.936476
16	0.001088	0.09621	0.98882*

Optimal outcome

Table 8: Lists of favorable and non-favorable attributes.

Attributes	Constraint	Comment
BSFC	Lower value	Favorable
BTE	Higher value	Favorable
CO	Lower value	Favorable
HC	Lower value	Favorable
CO_2	Lower value	Non- favorable
NOx	Lower value	Favourable

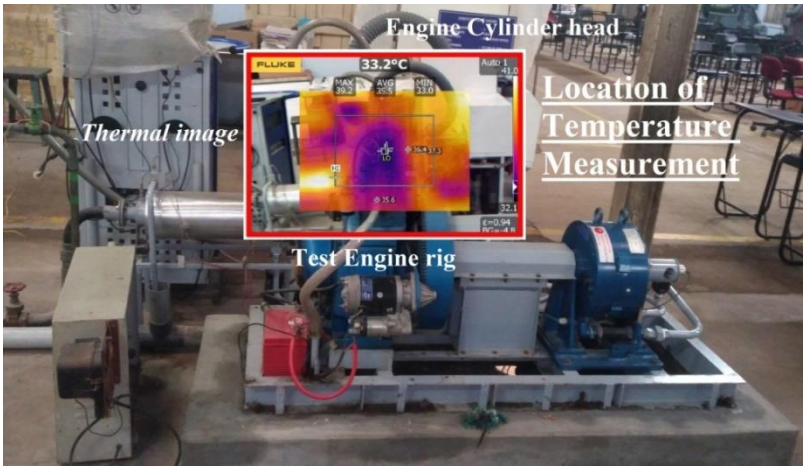

Fig. 13: Location of cylinder head temperature measurement.

metal oxide nanocatalyst enhanced the flame propagation and shortens the ignition delay by providing adequate oxygen to the fuel blends [46]. Therefore, F3 fuel delivers a superior engine response with lesser emissions compared to F0, F1 and F2. From the thermal images validation, an optimal fuel blend of F3 was elected at peak load condition, based on lower emission.

CONCLUSIONS

The objective of this experimental research is to accomplish the enhanced engine performance, to satisfy the energy needs. The present study considers engine load, AM pyrolysis oil neat blend and CuO nano additive AM bio-oil blends as engine control factors to attain better engine performance with lesser emission. From this investigation, the following conclusions are made

- The experimental results depict that, F3 blends deliver a higher BTE of 11.79% as compared to diesel. This is due to may be due to the enrichment of the fuel spray characteristics by oxygenated biofuel with metal oxide amalgamation, which in turn increased in BTE value.
- The lower BSFC value was obtained in F3 (0.32 kg/kW h) than F1 and F2 fuels. The existence of higher oxygen in the nano additive fuel blend provided the enhanced fuel property which lead to lower BSFC value.
- From the emission analysis, F3 fuel delivered the lesser CO (0.24%). The reason behind this lesser CO% is CuO nano catalyst supplies sufficient oxygen to the nano-bio-oil blend, which leads to complete combustion.
- The UHC (143 ppm), NOx (487 ppm) and augmented CO_2 (9.78%) were observed at a peak W condition as compared to diesel and other fuel blends. This is because of the complete combustion of oxygenated biofuels.
- The TOPSIS technique optimized the engine parameters with a greater RCC value of 0.988822. This indicates that the TOPSIS optimized results (w=100% and Fuel=F3 blend) were accurate with valid improvements. Engine emission properties are also validated by the thermography images.
- IR-thermal images ensure that the F3 fuels emit a lower amount of harmful emissions as compared to diesel. The experimental results, TOPSIS outcomes and

Test No.	W	B	Thermal Image	Temperature (°C)	Figure No.
1	25	F0	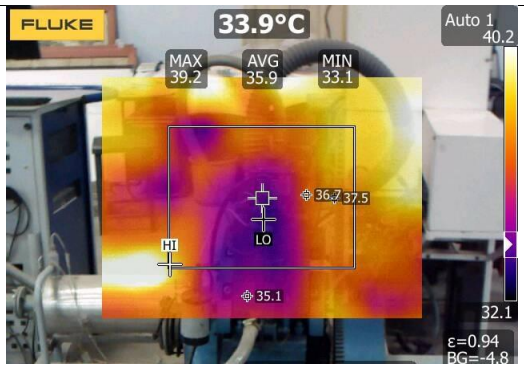	33.9	14.1
2	25	F1		33.7	14.2
3	25	F2		33.4	14.3
4	25	F3		33.2	14.4

Fig. 14: Thermography images.

Test No.	W	B	Thermal Image	Temperature (°C)	Figure No.
5	50	F0	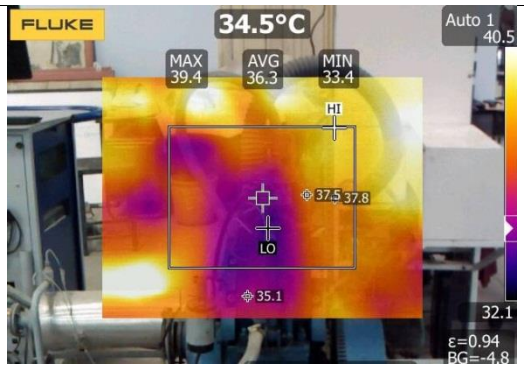	34.5	14.5
6	50	F1	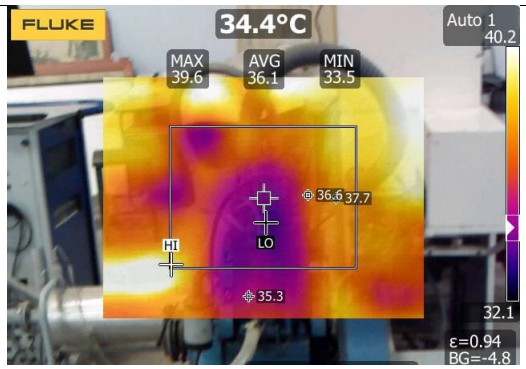	34.4	14.6
7	50	F2	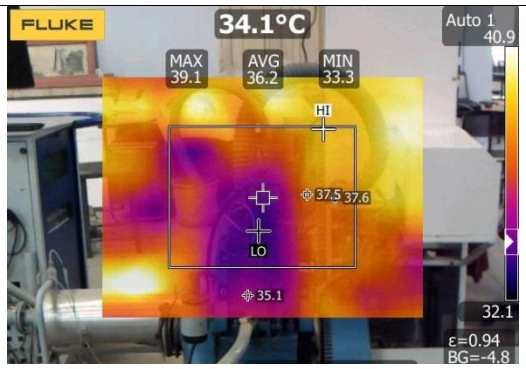	34.1	14.7
8	50	F3	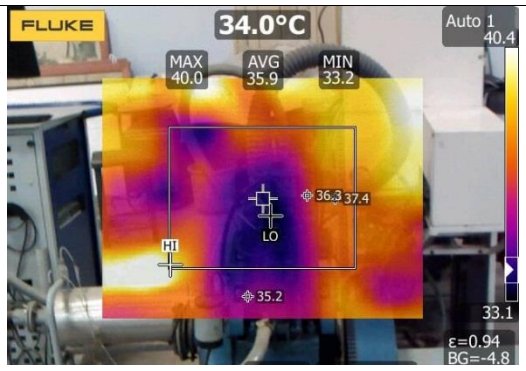	34.0	14.8

Fig. 14: Thermography images.

Test No.	W	B	Thermal Image	Temperature (°C)	Figure No.
9	75	F0	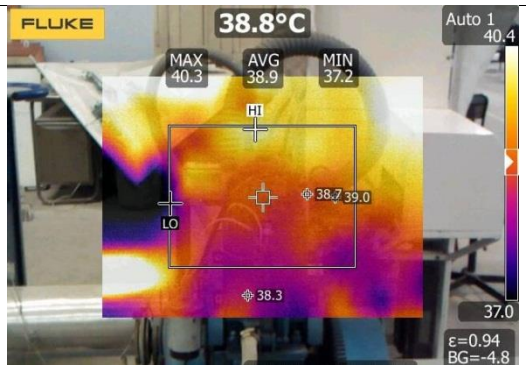	38.8	14.9
10	75	F1	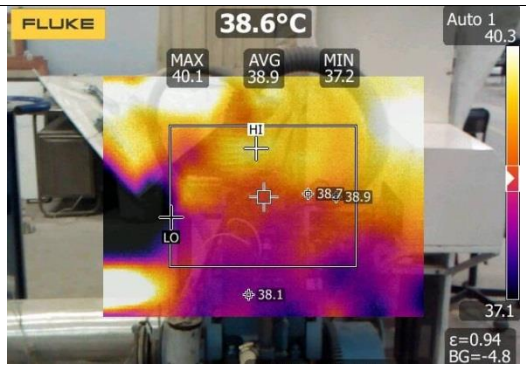	38.6	14.10
11	75	F2	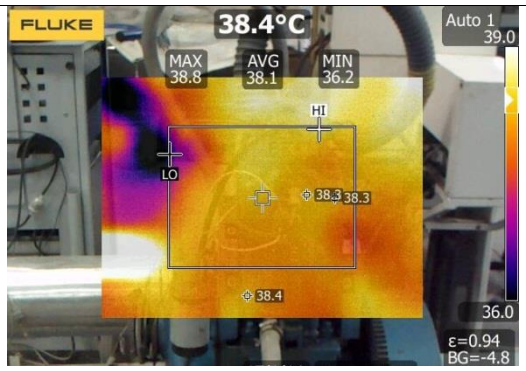	38.4	14.11
12	75	F3	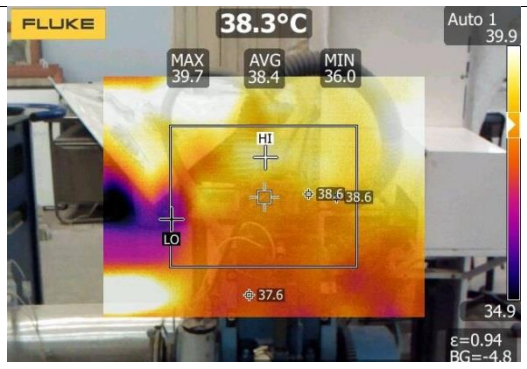	38.3	14.12

Fig. 14: Thermography images.

Test No.	W	B	Thermal Image	Temperature (°C)	Figure No.
13	100	F0	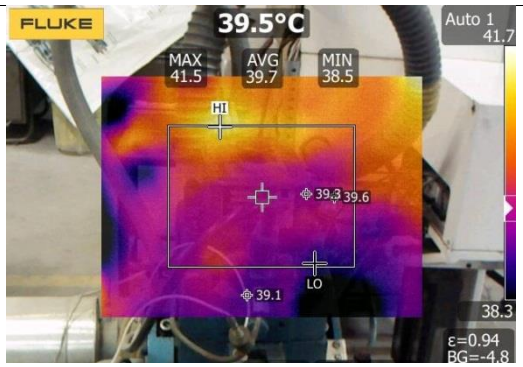	39.5	14.13
14	100	F1	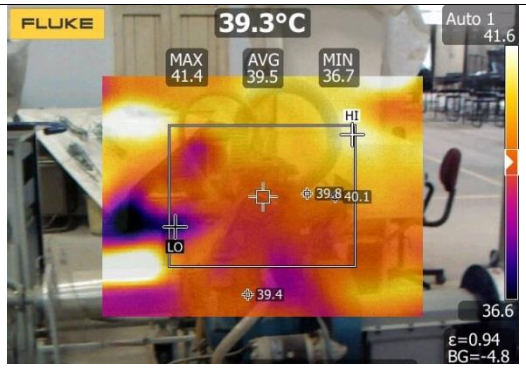	39.3	14.14
15	100	F2	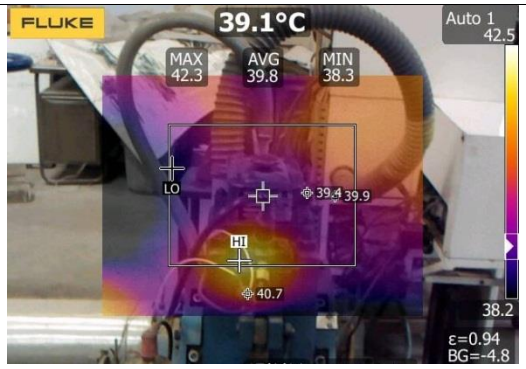	39.1	14.15
16	100	F3	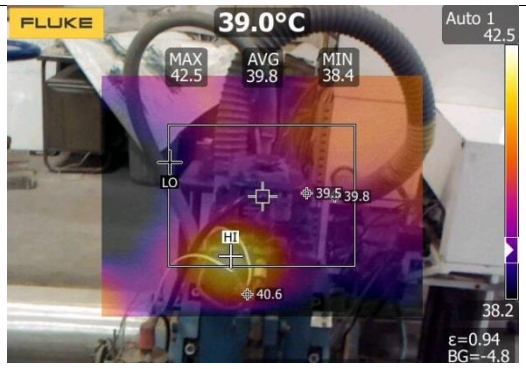	39.0	14.16

Fig. 14: Thermography images.

IR-thermal imager validation confirms that the F3 fuel is an optimal fuel blend concerning enriched performance and emissions compared to baseline diesel fuel.

Nomenclatures

AM	Aeglemarmelos
ASTM	American society for testing and materials
BSFC	Brake specific fuel consumption
BTE	Brake thermal efficiency
CeO_2	Cerium oxide
CI	Compression-Ignition
CO	Carbon monoxide
CO_2	Carbon dioxide
CN	Cetane number
CuO	Copper oxide
CV	Calorific value
Da	Decision matrix
EGR	Exhaust gas recirculation
F0	Diesel
F1	20% AM pyrolysis oil + 80% F0
F2	20% AM pyrolysis oil + 80% F0 + CuO 30 ppm
F3	20% AM pyrolysis oil + 80% F0 + CuO 50 ppm
IR	Infrared
IRT	Infrared thermography
MgO	Magnesium oxide
MODM	Multi-objective decision making
NIS	Negative ideal solution
NOx	Oxides of nitrogen
PIS	Positive ideal solution
Ppm	Parts per million
RCC	Relative closeness coefficient
TOPSIS	Technique for order preference by similarity to ideal solution
TIM	Thermal imager
UHC	Unburned Hydrocarbon
W	Engine load
Wj	Weighted value of each attribute
S_i^+	Positive separation measure
S_i^-	Negative separation measure
ϕij	Weighted normalized matrix
ϕ^+	Positive ideal solution
ϕ^-	Negative ideal solution
Δij	Normalization value of decision matrix

Received : Nov. 30, 2021 ; Accepted : Feb. 14, 2022

REFERENCES

[1] Sakthivel R., Ramesh K., Purnachandran R., Mohamed Shameer P., A Review on the Properties, Performance and Emission Aspects of the Third Generation Biodiesels, *Renewable and Sustainable Energy Reviews*, **82**: 2970-2992 (2018). https://doi.org/10.1016/j.rser.2017.10.037

[2] Fu P., Bai X., Yi W., Li Z., Li Y., Wang L., Assessment on Performance, Combustion and Emission Characteristics of Diesel Engine Fuelled with Corn Stalk Pyrolysis Bio-Oil/Diesel Emulsions with $Ce_{0.7}Zr_{0.3}O_2$ Nanoadditive, *Fuel Processing Technology*, **167**: 474-483 (2017). https://doi.org/10.1016/j.fuproc.2017.07.032

[3] Babu D., Anand R., Effect of Biodiesel-diesel-n-Pentanol and Biodiesel-diesel-n-hexanol Blends on Diesel Engine Emission and Combustion Characteristics, *Energy*, **133**: 761-776 (2017). https://doi.org/10.1016/j.energy.2017.05.103

[4] Kumaravel S. T., Murugesan A., Vijayakumar C., Thenmozhi M., Enhancing the Fuel Properties of Tyre Oil Diesel Blends by Doping Nano Additives for Green Environments, *Journal of Cleaner Production*, **240**: 118128 (2019). https://doi.org/10.1016/j.jclepro.2019.118128

[5] Baranitharan P., Ramesh K., Sakthivel R., Measurement of Performance and Emission Distinctiveness of Aegle Marmelos Seed Cake Pyrolysis Oil/Diesel/TBHQ Opus Powered in a DI Diesel Engine Using ANN and RSM, *Measurement*, **144**: 366-380 (2019). https://doi.org/10.1016/j.measurement.2019.05.037

[6] Rajamohan., Sakthivel., Ramesh Kasimani., Analytical Characterization of Products Obtained from Slow Pyrolysis of Calophyllum Inophyllum Seed Cake: Study on Performance and Emission Characteristics of Direct Injection Diesel Engine Fuelled with Bio-Oil Blends, *Environmental Science and Pollution Research*, **10**: 9523-9538 (2018). https://doi.org/10.1007/s11356-018-1241-x

[7] Ramakrishnan Purnachandran., Ramesh Kasimani., Mohamed Shameer Peer., Sakthivel Rajamohan., Assessment of n-pentanol/Calophyllum inophyllum/diesel Blends on the Performance, Emission, and Combustion Characteristics of a Constant-Speed Variable Compression Ratio Direct Injection Diesel Engine, *Environmental Science and Pollution Research*, **14**: 13731-13744 (2018). https://doi.org/10.1007/s11356-018-1566-5

[8] Mathimani T., Senthil Kumar T., Chandrasekar M., Uma L., Prabaharan D., Assessment of Fuel Properties, Engine Performance and Emission Characteristics of Outdoor Grown Marine Chlorella Vulgaris BDUG 91771 Biodiesel, *Renewable Energy*, **105**: 637-646 (2017). https://doi.org/10.1016/j.renene.2016.12.090

[9] Pradhan Debalaxmi., Harisankar Bendu., Singh R. K., Murugan S., Mahua Seed Pyrolysis Oil Blends as an Alternative Fuel for Light-Duty Diesel Engines, *Energy*, **118**: 600-612 (2017). https://doi.org/10.1016/j.energy.2016.10.091

[10] Hosseini S.H., Taghizadeh-Alisaraei A., Ghobadian B., Abbaszadeh-Mayvan A., Performance and Emission Characteristics of a CI Engine Fuelled with Carbon Nanotubes and Diesel-Biodiesel Blends, *Renewable Energy*, **111**: 201-213 (2017). https://doi.org/10.1016/j.renene.2017.04.013

[11] Dhinesh B., Annamalai M., A Study on Performance, Combustion and Emission Behaviour of Diesel Engine Powered by Novel Nano Nerium Oleander Biofuel, *Journal of Cleaner Production*, **196**: 74-83 (2018). https://doi.org/10.1016/j.jclepro.2018.06.002

[12] Chaichan M.T., Kadhum A.A. H., Al-Amiery A.A., Novel Technique for Enhancement of Diesel Fuel: Impact of Aqueous Alumina Nano-Fluid On Engine's Performance and Emissions, *Case Studies in Thermal Engineering*, **10**: 611-620 (2017). https://doi.org/10.1016/j.csite.2017.11.006

[13] Najafi G., Diesel Engine Combustion Characteristics Using Nano-Particles in Biodiesel-Diesel Blends, *Fuel*, **212**: 668-678 (2018). https://doi.org/10.1016/j.fuel.2017.10.001

[14] Karthikeyan S., Prathima A., Emission Analysis of the Effect of Doped Nano-Additives on Biofuel in A Diesel Engine, *Energy Sources, Part A: Recovery, Utilization, and Environmental Effects*, **24**: 3702-3708 (2016). https://doi.org/10.1080/15567036.2016.1166164

[15] Sharma S.K., Das R.K., Sharma A., Improvement in the Performance and Emission Characteristics of Diesel Engine Fueled with Jatropha Methyl Ester and Tyre Pyrolysis Oil by Addition of Nano Additives, *Journal of the Brazilian Society of Mechanical Sciences and Engineering*, **7**: 1907-1920 (2016). https://doi.org/10.1007/s40430-015-0454-x

[16] Sachuthananthan B., Krupakaran R.L., Balaji G., Exploration on the Behaviour Pattern of a DI Diesel Engine Using Magnesium Oxide Nano Additive with Plastic Pyrolysis Oil as Alternate Fuel, *International Journal of Ambient Energy*, **6**: 701-712 (2021). https://doi.org/10.1080/01430750.2018.1563812

[17] Gumus., Soner., Hakan Ozcan., Mustafa Ozbey., Bahattin Topaloglu., Aluminum Oxide and Copper Oxide Nanodiesel Fuel Properties and Usage in a Compression Ignition Engine, *Fuel*, **163**: 80-87 (2016). https://doi.org/10.1016/j.fuel.2015.09.048

[18] Tamilvanan A., Balamurugan K., Vijayakumar M., Effects of Nano-Copper Additive on Performance, Combustion and Emission Characteristics of Calophyllum Inophyllum Biodiesel in CI Engine, *Journal of Thermal Analysis and Calorimetry*, **1**: 317-330 (2019). https://doi.org/10.1007/s10973-018-7743-4

[19] Rajesh K., Devan P.K., Bharth Sai Kumar G. K., Parametric Optimization and Biodiesel Production from Coconut Fatty Acid Distillate, *Iranian Journal of Chemistry and Chemical Engineering*, **40(1)** : 343-355 (2021). 10.30492/IJCCE.2020.39119

[20] Gopinath Soundararajan., Devan P.K., Optimization and Prediction of Reaction Parameters of Plastic Pyrolysis Oil Production Using Taguchi Method, *Iranian Journal of Chemistry and Chemical Engineering (IJCCE)*, **39(2)** (2020). 10.30492/IJCCE.2020.33965

[21] Sudhagar S., Sakthivel M., Prince Mathew J., Ajith Arul Daniel S., A Multi Criteria Decision Making Approach for Process Improvement in Friction Stir Welding of Aluminium Alloy, *Measurement*, **108**: 1-8 (2017). https://doi.org/10.1016/j.measurement.2017.05.023

[22] Vinodh S., Govind Mulanjur., Arjun Thiagarajan., Sustainable Concept Selection Using Modified Fuzzy TOPSIS: A Case Study, *International Journal of Sustainable Engineering*, **2**: 109-116 (2013). https://doi.org/10.1080/19397038.2012.682100

[23] Paramasivam Baranitharan., Ramesh Kasimani., Sakthivel Rajamohan., Experimental Assessment and Multi-Response Optimization of Diesel Engine Performance and Emission Characteristics Fuelled with Aegle Marmelos Seed Cake Pyrolysis Oil-Diesel Blends Using Grey Relational Analysis Coupled Principal Component Analysis, *Environmental Science and Pollution Research*, **26(7)**: 6980-7004 (2019).
https://doi.org/10.1007/s11356-019-04164-8

[24] Baranitharan P., Ramesh K., Sakthivel R., Multi-Attribute Decision-Making Approach for Aegle Marmelos Pyrolysis Process Using TOPSIS and Grey Relational Analysis: Assessment of Engine Emissions Through Novel Infrared Thermography, *Journal of Cleaner Production*, **234**: 315-328 (2019).
https://doi.org/10.1016/j.jclepro.2019.06.188

[25] Paramasivam B., Somasundaram K., Selection of Smart Fuel Opus for Diesel Engine Depending on Their Fuel Characteristics: An Intelligent Hybrid Decision-Making Approach, *Environmental Science and Pollution Research*, **44**: 62216-62234 (2021).
https://doi.org/10.1007/s11356-021-14928-w

[26] Paramasivam B., Kumanan S., Kavimani V., Varatharajulu M., Fuzzy-based Prediction of Compression Ignition Engine Distinctiveness Powered by Novel Graphene Oxide Nanosheet Additive Diesel–Aegle Marmelos Pyrolysis Oil Ternary Opus, *International Journal of Energy and Environmental Engineering*, 1-19 (2022).
https://doi.org/10.1007/s40095-021-00458-1

[27] Paramasivam B., Fuzzy Prediction and RSM Optimization of CI Engine Performance Analysis: Aegle Marmelos Non-Edible Seed Cake Pyrolysis Oil as a Diesel Alternative, *Energy Sources, Part A: Recovery, Utilization, and Environmental Effect*, 1-17 (2020).
https://doi.org/10.1080/15567036.2020.1773971

[28] Anupam K., Shivhare Lal P., Bist V., Sharma A.K., Swaroop V., Raw Material Selection for Pulping and Papermaking Using TOPSIS Multiple Criteria Decision Making Design, *Environmental Progress & Sustainable Energy*, **3**: 1034-1041 (2014).
https://doi.org/10.1002/ep.11851

[29] Muniappan K., Rajalingam M., TOPSIS-Based Parametric Optimization of Compression Ignition Engine Performance and Emission Behavior with Bael Oil Blends For Different EGR and Charge Inlet Temperature, *Environmental Science and Pollution Research*, **19**: 19040-19053 (2018).
https://doi.org/10.1007/s11356-018-2048-5

[30] Madhu P., Nithiyesh Kumar Ch., Anojkumar L., Matheswaran M., Selection of Biomass Materials for Bio-Oil Yield: A Hybrid Multi-Criteria Decision Making Approach, *Clean Technologies and Environmental Policy*, **6**: 1377-1384 (2018).
https://doi.org/10.1007/s10098-018-1545-z

[31] Taheri-Garavand A., Ahmadi H., Omid M., Mohtasebi S.S., Mollazade K., Russell Smith A.J., Carlomagno G.M., An Intelligent Approach for Cooling Radiator Fault Diagnosis Based on Infrared Thermal Image Processing Technique, *Applied Thermal Engineering*, **87**:434-443 (2015).
https://doi.org/10.1016/j.applthermaleng.2015.05.038

[32] Paramasivam B, Investigation on The Effects of Damping over the Temperature Distribution on Internal Turning Bar Using Infrared Fusion Thermal Imager Analysis *via* Smartview Software, *Measurement*, **162**:107938 (2020).
https://doi.org/10.1016/j.measurement.2020.107938

[33] Ramesh K., Baranitharan P., Sakthivel R., Investigation of the Stability on Boring Tool Attached with Double Impact Dampers Using Taguchi Based Grey Analysis and Cutting Tool Temperature Investigation through FLUKE-Thermal Imager, *Measurement*, **131**: 143-155 (2019).
https://doi.org/10.1016/j.measurement.2018.08.055

[34] Baranitharan P., Kumanan S., Sudhagar S., An Intelligent Novel Approach for Diesel Engine Life Monitoring Using Infrared Image Processing Technic, *Environmental Progress & Sustainable Energy*, (2021).
http://dx.doi.org/10.1002/ep.13712

[35] Shameer P., Ramesh K., Experimental Evaluation on Performance, Combustion Behavior and Influence of In-Cylinder Temperature on NOx emission in a DI Diesel Engine Using Thermal Imager for Various Alternate Fuel Blends, *Energy*, **118**: 1334-1344 (2017).
https://doi.org/10.1016/j.energy.2016.11.017

[36] Shameer Peer M., Nishath Peer M., Experimental Investigation on Engine Characteristics Fueled with Waste HDPE Oil and Study on NOx Emission Variation Using Thermal Imager, *Environmental Science and Pollution Research*, **4**: 3436-3446 (2019).
https://doi.org/10.1007/s11356-018-3830-0

[37] Kıbar M.E., Akin A.N., Optimization of Carbon Dioxide Capture Process Parameters in Sodium Metaborate Solution, *Iranian Journal of Chemistry and Chemical Engineering (IJCCE)*, **40(5)**: 1554-1565 (2021).
10.30492/IJCCE.2020.40538

[38] Nwosu-Obieogu K., Aguele F.O., Chiemenem L., Optimization on Rubber Seed Oil Epoxidation Process Parameters Using Response Surface Methodology, *Iranian Journal of Chemistry and Chemical Engineering (IJCCE)*, **40**: 1575-1583 (2021).
10.30492/IJCCE.2020.40345

[39] Paramasivam Baranitharan., Ramesh Kasimani., Sakthivel Rajamohan., Characterization of Pyrolysis Bio-Oil Derived From Intermediate Pyrolysis of Aegle Marmelos De-Oiled Cake: Study on Performance and Emission Characteristics of CI Engine Fueled with Aegle Marmelos Pyrolysis Oil-Blends, *Environmental Science and Pollution Research*, **33**: 33806-33819 (2018).
https://doi.org/10.1007/s11356-018-3319-x

[40] Baranitharan P., Ramesh K., Sakthivel R., Analytical Characterization of the Aegle Marmelos Pyrolysis Products and Investigation on the Suitability of Bio-Oil as a Third Generation Bio-Fuel for CI Engine, *Environmental Progress & Sustainable Energy*, **38(4)**: 13116 (2019).
https://doi.org/10.1002/ep.13116

[41] Paramasivam B., Investigation and Improvement on Storage Stability of Pyrolysis Oil Obtained From Aegle Marmelos De-Oiled Seed Cake, *Energy Sources, Part A: Recovery, Utilization, and Environmental Effects*, **43(8)**: 953-967 (2021).
https://doi.org/10.1080/15567036.2019.1632989

[42] Baranitharan P., Exergy Analysis of A Diesel Engine Fuelled with Aegle Marmelos De-Oiled Seed Cake Pyrolysis Oil Opus, *Environmental Progress & Sustainable Energy*, **39(5)**: 13426 (2020).
https://doi.org/10.1002/ep.13426

[43] Shaafi T., Sairam K., Gopinath A., Kumaresan G., Velraj R., Effect of Dispersion of Various Nanoadditives on the Performance and Emission Characteristics of a CI Engine Fuelled with Diesel, Biodiesel And Blends—A Review, *Renewable and Sustainable Energy Review*, **49**: 563-573 (2015).
https://doi.org/10.1016/j.rser.2015.04.086

[44] Bibin Ch., Kumarasami Devan P., Gopinath S., Ramachandran T., Performance and Environmental Impact Assessment of Diesel Engine Operating on High Viscous Punnai Oil-Diesel Blends, *Environmental Science and Pollution Research*, (2022).
DOI: 10.21203/rs.3.rs-1152837/v1

[45] Chrysafi A. P., Athanasopoulos N., Siakavellas N. J., Damage Detection on Composite Materials with Active Thermography and Digital Image Processing, *International Journal of Thermal Sciences*, **116**: 242-253 (2017).
https://doi.org/10.1016/j.ijthermalsci.2017.02.017

[46] Kiran S., Sai., Madhu S., Chidambaranathan Bibin., Mebratu Markos Woldegiorgis., Kumran P., Effects of Chrysopogon Zizanioides Nano Additive with Palm Biodiesel on Engine Performance and Exhaust Emissions, *Materials Today: Proceedings*, **45**: 6951-6957 (2021).
https://doi.org/10.1016/j.matpr.2021.01.416

[47] Bibin C., Kannan P., Seeni, Devan P. K., Performance, Emission and Combustion Characteristics of a Direct Injection Diesel Engine Using Blends of Punnai Oil Biodiesel and Diesel as Fuel, *Thermal Science*, **24(1A)**: 13 (2020).
DOI:10.2298/TSCI180325233B

[48] Chidambaranathan Bibin., Gopinath S., Aravindraj R., Devaraj A., Gokula Krishnan S., Jeevaananthan J.K.S., the Production Of Biodiesel from Castor Oil as a Potential Feedstock and its Usage in Compression Ignition Engine: A Comprehensive Review, *Materials Today: Proceedings*, **33**: 84-92 (2020).
https://doi.org/10.1016/j.matpr.2020.03.205

[49] Venugopal P., Kasimani R., Chinnasamy S., Prediction and Optimization of CI Engine Performance Fuelled with Calophyllum Inophyllum Diesel Blend Using Response Surface Methodology (RSM), *Environmental Science and Pollution Research*, **25**: 24829-24844 (2018).
https://doi.org/10.1007/s11356-018-2519-8

[50] Soundararajan G., Ponnusamy Kumarasami D., Chidambaranathan B., Kasi Viswanathan P., Influence of Retarded Injection Timing on Thermal Performance and Emission Characteristics of a Diesel Engine Fuelled with an Optimized Pyrolytic Blend, *Energy & Environment*, **33(6):** 0958305X211033970 (2021).
https://doi.org/10.1177/0958305X211033970

[51] Rajamohan S., Thangamuthu M., Pandurangan G.K., Vivekanandan S., Ramadasan A., Optimization of Performance and Emission Characteristics of Compression Ignition Engine Powered with Azolla Pinnata Fuel Blends–A Response Surface Methodology Approach, *Energy Sources, Part A: Recovery, Utilization, and Environmental Effects*, 1-10 (2021).
https://doi.org/10.1080/15567036.2021.1923866